

## A novel fuzzy sliding mode control approach for chaotic systems

R. Khalili Amirabadi<sup>1</sup>, O. S. Fard<sup>2</sup> and A. Mansoori<sup>3</sup>

<sup>1,2,3</sup>*Department of Applied Mathematics, Faculty of Mathematical Sciences, Ferdowsi University of Mashhad, Mashhad, Iran*

roya.khalili.a@gmail.com; omidsfard@gmail.com; soleimani@um.ac.ir; am.ma7676@yahoo.com; a-mansoori@mail.um.ac.ir.

### Abstract

The purpose of this paper is to study the stabilization problem for a class of uncertain chaotic systems against unknown dynamics and disturbances, based on fuzzy sliding mode controller approaches. To fulfill this aim, the first- and the second-order sliding mode controllers and an adaptive variable universe fuzzy sliding mode controller are combined to a set of linguistic rules, to design some novel approaches for improving the performance of the control action and eliminating the chattering issue. The stability analysis of the closed-loop system is proved via the Lyapunov stability theorem, and also the convergence of the tracking error to zero in finite-time is guaranteed. The new proposed control laws contribute the control actions to outperform the conventional one in terms of chattering reduction and elimination, along with lessening in the reaching time. Moreover, some numerical simulations are provided to depict that the proposed control laws are not only robust with respect to uncertainties and external disturbances, which lead the system to the desired state, but also can significantly eliminate the chattering effect.

*Keywords:* Sliding mode controller, chaos, Takagi–Sugeno (T-S) fuzzy model, boundary layer variable, chattering.

## 1 Introduction

Over the past years, the control of the chaotic systems has been attracted widespread interest from a practical point of view in the science, engineering, and the theoretical value. Many researchers have paid attention to propose appropriated control algorithms to control the chaotic systems. Hitherto, various controller approaches have been designed to control this nonlinear ubiquitous phenomenon, such as the OGY method [25], feedback linearization [10], adaptive method [1], backstepping method [18], noisy synchronization method [43], sliding mode controller [7, 13, 21, 38], fuzzy control [4], fuzzy neural network control [44], passive control [42], and adaptive neuro-fuzzy inference system based control [11].

In the real world problems and in most practical systems, we always expect to encounter unknown model uncertainties. Among the above methods, the conventional (first-order) sliding mode control (SMC) is one of the useful robust controls due to its advantages including the fast response and low sensitivity to uncertainties and external disturbances. Nonetheless, the conventional SMC has the deficiency of the chattering phenomenon. Reducing the chattering phenomenon and the reaching time is a main issue when designing an SMC. To tackle these drawbacks, so far several approaches have been proposed, among which the boundary layer method [35, 41], dynamic sliding mode surface [20], global SMC [8], fuzzy SMC [3, 6, 14], and in particular, high-order sliding mode control (HOSMC) [23] (especially, second-order sliding mode control (SOSMC) [2]).

On the other hand, recently, some studies have endeavored to combine the mentioned methods for improving control performance. For example, Joo and Subramaniam [12, 28, 29] investigated the fuzzy integral sliding-mode control for permanent magnet synchronous generator-based wind energy conversion systems. In [33], the boundary layer technique was combined with a fuzzy logic control. Also, terminal sliding mode controller was combined into a fuzzy system to stabilize the equilibrium point of the system in [16]. Niu and Wang [24] proposed a variable universe fuzzy SMC to control a class of uncertain chaotic systems. In [39] an SMC based on a linear matrix inequality was proposed for chaotic systems. Van, Kang, and Suh [37] combined the Takagi–Sugeno (T-S) fuzzy model and the second-order sliding mode observer. In [17], a new sliding surface was defined based on a combination of the conventional sliding surface

in the terminal sliding mode control and a nonlinear function of the integral of the system states. Medhaffar, Feki, and Derbel [22] investigated the stabilization of unstable periodic orbits of continuous-time chaotic systems using fuzzy time-delayed controller. Likewise, Chang and Hsu [5] studied multiple performance constrained sliding mode fuzzy control problem for continuous-time stochastic nonlinear systems with multiplicative noises. In [9], a terminal SMC (TSMC) and the adaptive control techniques were combined to the states tracking error, which can attain the terminal sliding mode surface and converge to zero in a finite-time. Moreover, a TSMC was designed in [36] for multi-input, multi-output (MIMO) uncertain nonlinear systems in order to reduce the chattering phenomenon. Furthermore, a new backstepping control was merged with a super-twisting algorithm for MIMO nonlinear strict-feedback systems in [26]. Subramaniam, Song, and Joo [30] investigated the T-S fuzzy based SMC design of the discrete-time nonlinear model. Also, a sliding mode controller was utilized to overcome the adverse influences of stochastic packet dropouts in networked control systems in [27]. Moreover, fuzzy SMC for hyperchaotic Chen systems was investigated in [34].

Among the existing methods to improve the control performance, the developed fuzzy controller on the basis of the SMC system is a thought-provoking method that can simultaneously retain the benefits of the SMC and reduce the chattering effect. Indeed, the major features of the designed fuzzy controller decrease the fuzzy rules and relaxation of the uncertainty bound [15, 40]. In addition, the proper design of the fuzzy sliding mode controller is able to have a chattering reduction as well as increasing the tracking performance regarding the small uncertainties in the nonlinear system [32]. Recently, in [24], a variable universe adaptive fuzzy SMC was proposed and the control law was designed based on a set of linguistic rules.

The present work aims to consider different aspects of the fuzzy sliding mode controller along with whose stabilization for a specific class of uncertain chaotic system. To be laconic, we primarily introduce and investigate several modified fusing approaches based on the fuzzy SMC, the fuzzy surface-based SMC, the fuzzy sliding mode structure based on the boundary layer theory, and finally, the fuzzy second-order SMC. Furthermore, we attempt to improve the results of a recently published article [24]. To be precise, we improve the performance of a class of uncertain chaotic system and enhance the control accuracy by introducing the universe fuzzy control variable, so that the reaching time is significantly faster than the one in [24]. The proposed control laws are smooth without any overshoot where the tracing error reduces meaningfully. At that juncture, the developed control schemes are hired for a class of uncertain chaotic system, that is, the multi-scroll chaotic system with the nonlinear hysteresis, is applied to illustrate their abilities and advantages. By the previous discussion, the motivation and the advantages of the paper are summarized as follows:

- Developed approaches are fast-response compared to other methods.
- The presented approaches improve the performance of the system, which is reduced the tracing error of state variables.
- The control accuracy is enhanced in all presented approaches.
- The reaching time is significantly faster than the other methods in published articles.
- The proposed control laws are smooth without any overshoot.

The layout of this paper is organized as follows: In Section 2, the mathematical model for a class of uncertain chaotic systems with external disturbance is described. Moreover, a new fuzzy sliding mode controller is introduced, and the stability of the proposed schemes for the uncertain chaotic systems is analyzed. Then, in Section 3, some simulation results are presented to illustrate the implementation, effectiveness, and validation of the presented schemes. Also, we discuss and compare the simulation results in this section. Finally, Section 4 culminates the paper.

## 2 Problem statement and system description

In this research, we purpose to focus on the group of chaotic systems with uncertainty described as follows:

$$\begin{cases} \dot{x}_i(t) = x_{i+1}(t), & i = 1, \dots, n-1 \\ \dot{x}_n(t) = f(X, t) + \Delta f(X, t) + d(t) + u(t), \end{cases} \quad (1)$$

where  $X(t) = [x_1(t), x_2(t), \dots, x_n(t)]^T = [x(t), \dot{x}(t), \dots, x^{(n-1)}(t)]^T \in \mathbb{R}^n$  denotes the system state vector. Also,  $f(X, t) \in \mathbb{R}$  stands for a determined nonlinear function of  $X$  and  $t$ ,  $u(t) \in \mathbb{R}$  is the control input,  $\Delta f(X, t)$  is the uncertainty parameter, and  $d(t)$  denotes the disturbance term. Furthermore, it is assumed that two terms  $\Delta f(X, t)$  and  $d(t)$  are bounded, that is,  $|\Delta f(X, t)| \leq F_{\max} > 0$  and  $|d(t)| \leq D_{\max} > 0$ . In fact, the main problem is to

design a control law that provides the desired performance for the uncertain chaotic system. Let the desired output be  $X_d(t) = [x_{d1}(t), x_{d2}(t), \dots, x_{dn}(t)]^T = [x_d(t), \dot{x}_d(t), \dots, x_d^{(n-1)}(t)]^T$ , and also assume that

$$E(t) = X(t) - X_d(t) = [e_1(t), e_2(t), \dots, e_n(t)]^T, \quad (2)$$

is the tracking errors vector of the variable  $X$  that  $e_{i+1} = \dot{e}_i$ ,  $i = 1, \dots, n - 2$ . Here, the target of the attitude control design is to offer an appropriate and novel fuzzy sliding mode controller, which guarantees that the output vector,  $X(t)$ , tracks the desired signal  $X_d(t)$ , that is,

$$\lim_{n \rightarrow \infty} \|E(t)\| = \lim_{n \rightarrow \infty} \|X(t) - X_d(t)\| \rightarrow 0. \quad (3)$$

To achieve this goal, which is, in fact, designing adequate control laws, this work deals with two major steps for the uncertain chaotic system in subsequent. The first step is to select a suitable sliding surface for the system such that the error vector converges to zero. The second one is to propose some new designed fuzzy controllers according to the SMC approaches to reduce the chattering phenomenon in the given system with inherent uncertainties and external disturbances.

A time-varying sliding surface in the state-space  $\mathbb{R}^n$  is introduced as follows:

$$s(t) = \left(\frac{d}{dt} + \lambda\right)^{n-1} e(t) = e_n(t) + \lambda_{n-1} e_{n-1} + \lambda_{n-2} e_{n-2} + \dots + \lambda_1 e_1 = e_n(t) + \sum_{i=1}^{n-1} \lambda_i e_i(t), \quad (4)$$

where  $\lambda_i$ ,  $i = 1, \dots, n - 1$  are the sliding surface coefficients that can be chosen such that the surface is strictly Hurwitz. After designing the appropriate sliding surface, now, we need to give a control law such that any state  $X$  outside of the sliding surface  $s(t) = 0$  is driven to reach the surface in the finite-time. By solving  $\dot{s}(t) = 0$ , that is,

$$\dot{s}(t) = \dot{e}_n(t) + \sum_{i=1}^{n-1} \lambda_i \dot{e}_i(t) = 0, \quad (5)$$

the control law can be obtained, which is so-called the equivalent control  $u_{eq}$ . Since in a real world system, the uncertainty and external disturbance,  $\Delta f(X, t)$  and  $d(t)$ , are unknown, in the equivalent control, these terms are ignored. Hence, by substituting (1) with (4), the equivalent control  $u_{eq}$  is determined as

$$u_{eq} = -f(X, t) - \sum_{i=1}^{n-1} \lambda_i e_{i+1} + x_d^{(n)}(t). \quad (6)$$

In the conventional SMC, the control law is selected as follows:

$$u = u_{eq} - K u_{reach}, \quad (7)$$

where the reaching control,  $u_{reach}$ , is

$$u_{reach} = \text{Sign}(s). \quad (8)$$

Moreover,  $K$  is called the control gain, which is positive and  $\text{Sign}(s(\cdot))$  is the Sign function of  $s(t)$ , that is,

$$\text{Sign}(s(t)) = \begin{cases} 1 & \text{if } s(t) > 0, \\ 0 & \text{if } s(t) = 0, \\ -1 & \text{if } s(t) < 0. \end{cases}$$

From (8) and (7), the overall control  $u$  is obtained as

$$u = u_{eq} - K \text{Sign}(s). \quad (9)$$

To obtain the convergence of  $X(t)$  to zero, we have to steer the sliding surface  $s$  in (2) to zero in the finite-time. This task can be achieved by applying Lyapunov function techniques. A candidate Lyapunov function is introduced as follows:

$$V = \frac{1}{2} s^2. \quad (10)$$

Therefore, to guarantee that the trajectory of the system in (1) is driven toward the sliding surface in (4) and remains on it thereafter, a sufficient condition is

$$\dot{V} = s\dot{s} \leq -\zeta V^\tau, \quad (11)$$

where  $\zeta$  is a strictly positive constant and  $0 < \tau < 1$ . Equation (11) is so-called the reaching condition. In (9), the discontinuous term in the control law results in the chattering phenomenon that can affect the unmodeled system dynamics and cause system instability. It is necessary noting that to gain an ideal performance, the chattering must be eliminated. As mentioned before, in fact, there are different methods suggested to reduce the chattering phenomenon in the traditional SMC such as the boundary layer solution, observer-based solution, higher order SMC, and fuzzy control solution. However, according to [35], to reduce the chattering effects, we first need to define a thin boundary layer neighboring the switching surface  $B(t) = \{e(t) | s(e(t)) \leq \varphi\}$ , where  $\varphi > 0$  is so-called the boundary layer thickness. Hence, by smoothing out the discontinuity in  $B(t)$ , we may expect to weaken the chattering effectively. To this end, outside of  $B(t)$ , we choose the control law,  $u(t)$  by (9), and inside  $B(t)$ , we replace the term  $\text{Sign}(s)$  by  $s/\varphi$  in (9) to determine the control law. This process guarantees that the boundary layer is always attractive (for more details, we refer the interested readers to [35]). Actually, the  $\text{Sign}$  function in (9) is replaced by the saturation function  $\text{Sat}(\cdot)$ , and accordingly, the reaching control is converted to  $u_{reach} = -K\text{Sat}(\frac{s}{\varphi})$ , where

$$\text{Sat}\left(\frac{s}{\varphi}\right) = \begin{cases} \frac{s}{\varphi} & \text{if } |s| \leq |\varphi| \\ \text{Sign}(s) & \text{if otherwise,} \end{cases} \quad (12)$$

is the saturation function, which will satisfy the reaching condition in (11). In this case, the modified control law becomes as follows:

$$u = e_{eq} - \bar{K}\text{Sat}\left(\frac{s}{\varphi}\right), \quad (13)$$

where  $\bar{K} = K - \varphi$ . On the other hand, another technique to tackle the chattering phenomenon is using the function  $\tanh(cs)$  instead of the function  $\text{Sign}(s)$  in (9) and consequently  $\tanh(\frac{s}{\varphi})$  instead of  $\text{Sat}(\frac{s}{\varphi})$  in (13), where  $c$  is a positive constant parameter. The response of the function  $\tanh(cs)$  with different values for  $c$ , the  $\text{Sat}$  function, and the  $\text{Sign}$  function is depicted in Fig. 1 from [2]. Note that, by increasing the value of  $c$ , the behavior of the function  $\tanh(cX)$  will be more similar to  $\text{Sign}(X)$ . Now, we are ready to propose some novel schemes to obtain a better performance, reducing

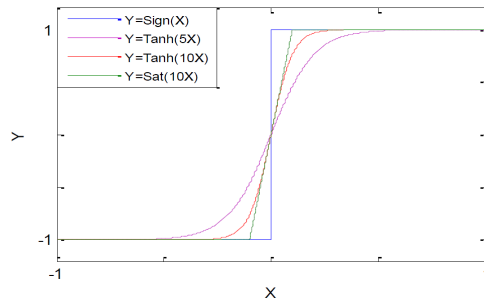


Figure 1: The response of  $\text{Sign}(\cdot)$ ,  $\text{Sat}(\cdot)$ , and  $\tanh(\cdot)$  functions

the chattering phenomenon significantly and efficiently, by a set of linguistic rules based on the expert knowledge and various sliding mode controllers. Next Lemma gives the sufficient conditions for finite-time stability for the equilibrium point of the system.

**Lemma 2.1.** [31] Consider the system  $\frac{dx}{dt} = f(x)$ ,  $f(0) = 0$ , and  $x \in \mathbb{R}^n$ , if there is a positive definite continuous function  $V(x)$  that satisfies  $\frac{dV}{dt} \leq -\zeta V^\tau$ , where the real numbers  $\zeta$  and  $\tau$  satisfy  $\zeta > 0$  and  $0 < \tau < 1$ , respectively, then  $V(x) = 0$  can be reached in finite-time  $t_{reach}$ , and the origin is a finite-time stable equilibrium of the system.

### 3 Traditional SMC and fuzzy control

In this section, several control laws are investigated in order to improve the performance of the control action for a class of chaotic systems. First, we consider traditional SMCs such as the boundary layer SMC that are combined with

the fuzzy logic control based on the T-S fuzzy rules, as mentioned in Approach A. Then by using the universe fuzzy control variable, we propose a new control law based on the fuzzy surface SMC, explained in Approach B. Afterwards Approaches A and B are combined and declared in Approach C.

### 3.1 Approach A.

In this approach, we use a fuzzy SMC based on the variable time boundary layer (FBSMC) surrounding the sliding surface to attenuate the chattering phenomenon for a class of chaotic systems with uncertainties and external disturbances. The FBSMC scheme is exhibited in Fig. 2. The fuzzy inference system in this case is a single-input-single-output. It

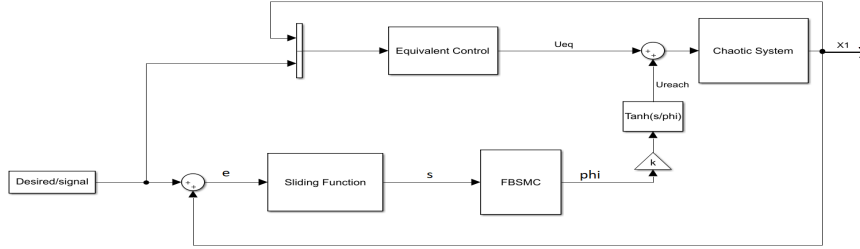


Figure 2: Scheme of the FBSMC

contains an equivalent control part and a single-input-single-output FBSMC. The sliding surface  $s$  is as the input linguistic variable of the FBSMC and  $\Phi_{fs}$  is as the output of the FBSMC and the error state is as the input of the sliding mode function. Therefore, regarding the universal approximation theorem [19], the universe fuzzy control variable can be shown as follows:

$$\Phi_{fs} = FBSMC(s). \tag{14}$$

The thickness of the boundary layer can be modified according to the sliding surface changes as the input, on the interval  $[0, a]$ . Therefore, the T-S fuzzy model with nine rules is used. The sets  $S_1, S_2, \dots, S_9$  are the fuzzy sets on the common interval  $[-a, a]$ , which are represented by language values “negative very big (NVB)”, “negative big (NB)”, “negative medium (NM)”, “negative small (NS)”, “zero (Z)”, “positive small (PS)”, “positive medium (PM)”, “positive big (PB)”, and “positive very big (PVB)”.

**Remark 3.1.** In this study, for the sake of convenience, we choose the interval  $[-1,1]$  to specify fuzzy sets. Moreover, all corresponding membership functions to the fuzzy sets are defined by “triangular membership functions” which are shown in Fig. 3. Also, the thickness of the boundary layer is fitting according to the changes of sliding surface. Therefore, it can change in interval  $[0,1]$ . In this work, we chose the following value as illustrated in Fig. 4.

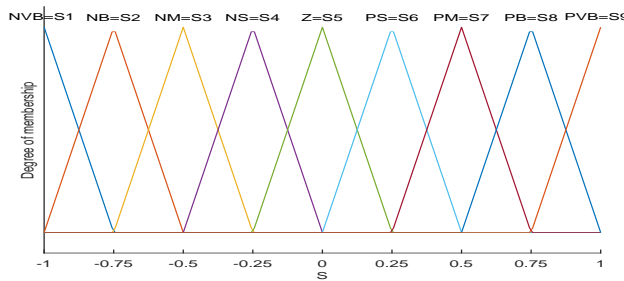


Figure 3: Input membership function for the FBSMC

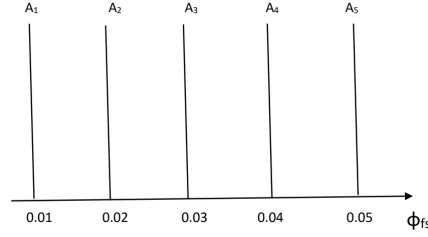


Figure 4: Output membership function for the FBSMC

In summary, the fuzzy SMC law is described as follows:

$$u = -f(X, t) - \sum_{i=1}^{n-1} \lambda_i e_{i+1} + x_d^{(n)}(t) - \bar{K} \tanh\left(\frac{s}{\Phi_{fs}}\right), \quad (15)$$

$$\Phi_{fs} = FBSMC(s) = \sum_{i=1}^9 S_i(s). \quad (16)$$

The fuzzy IF-THEN  $i$ th rule based on  $s$  is stated as follows:

IF  $s$  is  $S_i$  THEN  $\varphi_i = s + A_i s$ ,

where  $A = [A_i]_{i=1}^9$  is given as,

$$A = [A_5 \ A_4 \ A_3 \ A_2 \ A_1 \ A_2 \ A_3 \ A_4 \ A_5]. \quad (17)$$

Fig. 4 depicts the output membership function for the FBSMC. As a matter of fact, a basic consideration is used to determine the fuzzy rules as follows.

### Assumptions 1.

1. When the value of the sliding variable  $s$  is large in terms of absolute, a large number of the boundary layer thickness is selected.
2. When the value of the sliding variable  $s$  is small in terms of absolute, a small number of the boundary layer thickness is selected.

In the following theorem, we prove that the scheme in (15) is able to drive the chaotic system in (1) into the sliding surface  $s(t) = 0$ , that is, the reaching condition  $s\dot{s} < 0$  is guaranteed. Algorithm 1 demonstrates the summery of design procedure for the FBSMC.

---

#### Algorithm 1 (Algorithm for Approach A)

---

- 1: Determine a stable sliding mode surface from (4).
  - 2: Determine the implemented equivalent control from (6).
  - 3: Design the singleton-type FBSMC using  $s$ .
  - 4: Calculate the overall control  $u$  from (15).
- 

**Theorem 3.2.** Assume that the uncertain chaotic system in (1) is controlled by  $u$  in (15), where  $\Phi_{fs}$  is defined in (16) and  $K > F_{\max} + D_{\max} + \Phi_{fs}$ . Then, the error state trajectory converges to the sliding surface  $s(t) = 0$ . Moreover, the states of system in (1) converge to zero in finite-time.

*Proof.* A candidate Lyapunov function of the system is taken  $V = \frac{1}{2}s^2$ . Therefore  $\dot{s} = \sqrt{2V}^{\frac{1}{2}}$  Then to provide the

global finite-time stability, the condition  $\dot{V} < 0$  must be satisfied

$$\begin{aligned}
\dot{V} &= s\dot{s} = s[\dot{e}_n(t) + \sum_{i=1}^{n-1} \lambda_i \dot{e}_i] \\
&= s[f(X, t) + \Delta f(X, t) + d(t) + u_{eq}(t) - \bar{K} \tanh\left(\frac{s}{\Phi_{fs}}\right) - x_d^{(n)}(t) + \sum_{i=1}^{n-1} \lambda_i \dot{e}_i] \\
&= s[\Delta f(X, t) + d(t) - \bar{K} \tanh\left(\frac{s}{\Phi_{fs}}\right)] \\
&\leq |s|[\Delta f(X, t) + d(t) - \bar{K} \tanh\left(\frac{s}{\Phi_{fs}}\right)] \\
&\leq F_{\max}|s| + D_{\max}|s| - \bar{K}|s| \\
&= (F_{\max} + D_{\max} - K + \Phi_{fs})|s| \\
&= -(K - (F_{\max} + D_{\max} + \Phi_{fs}))|s| \\
&= -(K - (F_{\max} + D_{\max} + \Phi_{fs}))\sqrt{2}V^{\frac{1}{2}}
\end{aligned}$$

If we select  $K > F_{\max} + D_{\max} + \Phi_{fs}$  the condition  $\dot{V} \leq -\zeta V^{\frac{1}{2}}$  is satisfied, where  $\zeta = (K - (F_{\max} + D_{\max} + \Phi_{fs}))\sqrt{2}$ . By integrating from equation  $\dot{V} \leq -\zeta V^{\frac{1}{2}}$  between  $t_0 = 0$  and  $t = t_{reach}$  we have the following result,

$$t_{reach} \leq \frac{2}{\zeta}[V(t_0)]^{1/2}.$$

Thus, in accordance with Lemma 2.1, the states of chaotic system in (1) converge to zero in finite-time.  $\square$

### 3.2 Approach B.

The second approach to reduce the chattering issue is to use a fuzzy surface sliding mode control (FSSMC). In this case,  $I_i = [-E_i, E_i]$ ,  $i = 1, 2, \dots, n$  are, respectively, the interval of the input variables  $e_1, e_2, \dots, e_n$  of the FSSMC and  $J = [-S, S]$  is the interval of the output variables FSSMC. In this way, we will use the T-S fuzzy with the two-input-single-output fuzzy model, which has been widely utilized to model the nonlinear systems. In general, the fuzzy control rules according to the inputs and the output linguistic variable can be shown as follows:

$$S_{fs} = FSSMC(e_1, e_2, \dots, e_n). \quad (18)$$

In this approach, first we focus on the special case  $n = 2$  as:

$$S_{fs} = FSSMC(e_1, \dot{e}_1). \quad (19)$$

In Table 1, the values show the peak points of the fuzzy sets on the output interval. The sets  $\tilde{E}_1, \tilde{E}_2, \dots, \tilde{E}_9$  are the fuzzy sets on the common interval  $[-1, 1]$ , which are represented by the values of “negative very big”, “negative big”, “negative medium”, “negative small”, “zero”, “positive small”, “positive medium”, “positive big”, and “positive very big”. Also,  $\dot{\tilde{E}}_1, \dot{\tilde{E}}_2, \dots, \dot{\tilde{E}}_9$  are the fuzzy sets on the common interval  $[-1, 1]$ , which are again represented by the language values with the same meaning as above. All the membership functions of the fuzzy sets are similarly chosen as the “triangle membership functions”. Hence, the fuzzy SMC law is described as follows:

$$u = -f(X, t) - (\lambda e_1 + \dot{e}_1) + \ddot{x}_d(t) - K \tanh(S_{fs}), \quad (20)$$

where

$$\begin{aligned}
S_{fs} &= \sum_{i=1}^9 \sum_{j=1}^9 h_{ij} C_{ij} = FSSMS(e_1, \dot{e}_1) = GS(GE.e_1 + GCE.\dot{e}_1) = \lambda e_1 + \dot{e}_1 \\
h_{ij} &= \frac{\tilde{E}_{1i}(e_1) \dot{\tilde{E}}_{2j}(\dot{e}_1)}{\tilde{E}_{1i}(e_1) + \dot{\tilde{E}}_{2j}(\dot{e}_1)} \quad \text{for } i, j = 1, \dots, 9.
\end{aligned} \quad (21)$$

Here,  $GE$  (gain of error) is a scalar,  $GS = \lambda/GE$  and  $GCE = 1/GS$  for any given  $\lambda > 0$ , and  $C_{ij}$  is the membership function of the output. The FSSMC plant is illustrated in Fig. 5. It contains an equivalent control part and a two-input-single-output FSSMC. The error state  $e$  and its change rate  $\dot{e}$  are the input linguistic variables of the FSSMC, and  $S_{fs}$  is the output linguistic variable.

Fig. 6 depicts the output membership function for the FSSMC. Now, we consider the following assumptions.

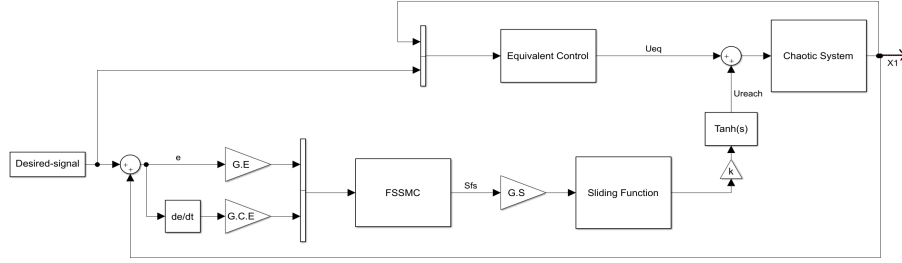


Figure 5: Scheme of the FSSMC

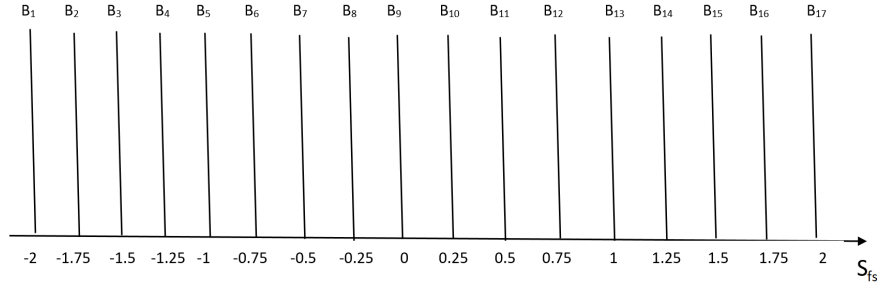


Figure 6: Output membership function for the FSSMC

### Assumptions 2.

Since the control inputs are selected from the common interval  $[-1, 1]$ , according to (5), the value of the outputs are chosen from the interval  $[-2, 2]$ .

1. When the error variable  $e_1$  and its derivative  $\dot{e}_1$  are negative very big, in order to decrease the quantity of  $e_1$  and  $\dot{e}_1$  for come back trajectory to reach the sliding surface, according to the definitions of the error and the sliding surface, the maximum value of the control output is required.
2. When the error variable  $e_1$  is positive very big and its derivative  $\dot{e}_1$  is negative very big, the control output value is zero.
3. When the error variable  $e_1$  and its derivative  $\dot{e}_1$  are positive very big, the maximum value of the control output is required for come back trajectory to reach the sliding surface.
4. In other modes, the control output is chosen proportional to the error variable  $e_1$  and its derivative  $\dot{e}_1$ , so that the convergence to the sliding surface takes place faster.

Regarding to Assumptions 2, we define the  $(i, j)$ th fuzzy rule, based on  $e_1$  and  $\dot{e}_1$  as follows:

IF  $e$  is  $\tilde{E}_i$  and  $\dot{e}_1$  is  $\dot{\tilde{E}}_j$  THEN  $s$  is  $C_{i,j}$ ,

where  $C_{i,j}$  is the  $(i, j)$ th element in Table 1. For instance,  $C_{3,6} = B_8$  and  $C_{7,8} = B_{14}$ .

Algorithm 2 demonstrates the summary of design procedure for the FSSMC.

---

### Algorithm 2 (Algorithm for Approach B)

---

- 1: Determine a stable sliding mode surface from (4).
  - 2: Determine the implemented equivalent control from (6).
  - 3: Design the singleton-type FSSMC using  $e_1$  and  $\dot{e}_1$ .
  - 4: Calculate the overall control  $u$  from (20).
-



Table 1: Rule-table of FSSMC

	$\tilde{E}_1$	$\tilde{E}_2$	$\tilde{E}_3$	$\tilde{E}_4$	$\tilde{E}_5$	$\tilde{E}_6$	$\tilde{E}_7$	$\tilde{E}_8$	$\tilde{E}_9$
$\tilde{E}_1$	$B_1$	$B_2$	$B_3$	$B_4$	$B_5$	$B_6$	$B_7$	$B_8$	$B_9$
$\tilde{E}_2$	$B_2$	$B_3$	$B_4$	$B_5$	$B_6$	$B_7$	$B_8$	$B_9$	$B_{10}$
$\tilde{E}_3$	$B_3$	$B_4$	$B_5$	$B_6$	$B_7$	$B_8$	$B_9$	$B_{10}$	$B_{11}$
$\tilde{E}_4$	$B_4$	$B_5$	$B_6$	$B_7$	$B_8$	$B_9$	$B_{10}$	$B_{11}$	$B_{12}$
$\tilde{E}_5$	$B_5$	$B_6$	$B_7$	$B_8$	$B_9$	$B_{10}$	$B_{11}$	$B_{12}$	$B_{13}$
$\tilde{E}_6$	$B_6$	$B_7$	$B_8$	$B_9$	$B_{10}$	$B_{11}$	$B_{12}$	$B_{13}$	$B_{14}$
$\tilde{E}_7$	$B_7$	$B_8$	$B_9$	$B_{10}$	$B_{11}$	$B_{12}$	$B_{13}$	$B_{14}$	$B_{15}$
$\tilde{E}_8$	$B_8$	$B_9$	$B_{10}$	$B_{11}$	$B_{12}$	$B_{13}$	$B_{14}$	$B_{15}$	$B_{16}$
$\tilde{E}_9$	$B_9$	$B_{10}$	$B_{11}$	$B_{12}$	$B_{13}$	$B_{14}$	$B_{15}$	$B_{16}$	$B_{17}$

**Remark 3.3.** In accordance with the previous discussion, we can consider the suggested linearization for the general case in (18) as follows:

$$S_{f_s} = FSSMC(e_1, e_2, \dots, e_n) = e_n + \sum_{i=1}^{n-1} \lambda_i e_i.$$

Now, we are able to prove the following theorem, which guarantees the reaching condition  $s\dot{s} < 0$ .

**Theorem 3.4.** Assume that the uncertain chaotic system in (1) is controlled by  $u$  in (20), where  $S_{f_s}$  is defined in (21) and  $K > F_{\max} + D_{\max}$ . Then, the error state trajectory converges to the sliding surface  $S_{f_s}(t) = 0$  in a finite-time. Moreover, the states of system in (1) converge to zero in finite-time.

*Proof.* A candidate Lyapunov function of the system is taken  $V = \frac{1}{2}S_{f_s}^2$ . Then, to provide the global finite-time stability, the condition  $\dot{V} \leq 0$  must be satisfied

$$\begin{aligned} \dot{V} &= S_{f_s} \dot{S}_{f_s} = S_{f_s} [\dot{e}_n + \sum_{i=1}^{n-1} \lambda_i \dot{e}_i] \\ &= S_{f_s} [f(X, t) + \Delta f(X, t) + d(t) + u_{eq}(t) - K \tanh(S_{f_s}) - x_d^{(n)}(t) + \sum_{i=1}^{n-1} \lambda_i \dot{e}_i] \\ &= S_{f_s} [\Delta f(X, t) + d(t) - \bar{K} \tanh(S_{f_s})] \\ &\leq |S_{f_s}| [|\Delta f(X, t) + d(t) - \bar{K} \tanh(S_{f_s})|] \\ &\leq F_{\max} |S_{f_s}| + D_{\max} |S_{f_s}| - K |S_{f_s}| \\ &= (F_{\max} + D_{\max} - K) |S_{f_s}| \\ &= -(K - (F_{\max} + D_{\max})) |S_{f_s}| \\ &= -(K - (F_{\max} + D_{\max})) \sqrt{2} V^{\frac{1}{2}}. \end{aligned}$$

Suppose  $K > F_{\max} + D_{\max}$ , and also, assume that  $t_{reach}$  is the time required to hit the sliding surface  $S_{f_s}(t) = 0$ . Integrating  $\dot{V} = S_{f_s}(t) \dot{S}_{f_s}(t) \leq -\zeta V^{\frac{1}{2}}$ , where  $\zeta = (K - (F_{\max} + D_{\max})) \sqrt{2}$  between  $t_0 = 0$  and  $t = t_{reach}$  leads to the following result:

$$\int_{t_0}^{t_{reach}} \frac{dV}{V^{\frac{1}{2}}} \leq \int_{t_0}^{t_{reach}} -\zeta dt.$$

Hence,  $t_{reach}$  is rewritten as follows:

$$t_{reach} \leq \frac{2}{\zeta} [V(t_0)]^{\frac{1}{2}},$$

Note that  $S_{f_s}(t_{reach}) = 0$ . Thus, in accordance with Lemma 2.1, the states of chaotic system in (1) converge to zero in finite-time.  $\square$

### 3.3 Approach C.

Here, to improve the performance of the two approaches, namely, A and B, we intend to merge two schemes FBSMC and FSSMC. First, we consider the variables  $e$  and  $\dot{e}$  as two inputs for the schemes including FBSMC (i.e., (21)) and we obtain the output  $S_{fs}$ . Then, by using  $S_{fs}$  as the input to the scheme FBSMC (i.e., (16)), consequently we have the output  $\Phi_{fs}$ . Hence, the fuzzy surface boundary sliding mode control law (FSBSMC) is defined as below:

$$u = -f(X, t) - \sum_{i=1}^{n-1} \lambda_i e_{i+1} + x_d^{(n)}(t) - \bar{K} \tanh\left(\frac{S_{fs}}{\Phi_{fs}}\right). \quad (22)$$

The plant FSBSMC is shown in Fig. 7. It shows an equivalent control part and a two-input-single output FSBSMC, where the error state  $e$  and its change rate  $\dot{e}$  are the input linguistic variables of the FSSMC,  $S_{fs}$  is the output of the FSSMC,  $S_{fs}$  is the input linguistic variable of the FBSMC, and  $\Phi_{fs}$  is the output of the FBSMC. Algorithm 3

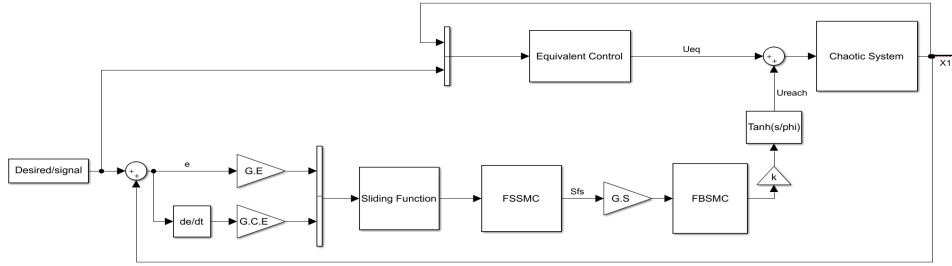


Figure 7: Scheme of the FSBSMC

demonstrates the summary of design procedure for the FSSMC.

---

#### Algorithm 3 (Algorithm for Approach C)

---

- 1: Determine a stable sliding mode surface from (4).
  - 2: Determine the implemented equivalent control from (6).
  - 3: Design the singleton-type FSSMC using  $e$  and  $\dot{e}$ .
  - 4: Design the singleton-type FBSMC using  $S_{fs}$ .
  - 5: Calculate the overall control  $u$  from (22).
- 

**Theorem 3.5.** Assume that the uncertain chaotic system in (1) is controlled by  $u$  in (22), where  $S_{fs}$  is defined in (21),  $\Phi_{fs}$  is as (16), and  $K > F_{\max} + D_{\max} + \Phi_{fs}$ . Then, the error state trajectory converges to the sliding surface  $S_{fs}(t) = 0$  in a finite-time. Moreover, the states of system in (1) converge to zero in finite-time.

*Proof.* The proof is similar to that of the preceding theorems. □

## 4 SOSMC and fuzzy control

As known, the SOSMC is a class of methods to reduce the chattering phenomenon. In this section, first we focus on a special case of SOSMC in which the super twist algorithm is agglutinated with the fuzzy logic control, and we provide Approach D. In this method, the  $\text{Sign}(\cdot)$  is used in the control law. Thereupon, with the purpose of improving the control action, this function is replaced with  $\tanh(\cdot)$ , which is expressed in Remark 4.2.

### 4.1 Approach D.

As we know, the main purpose of the conventional SMC is to keep the sliding variable  $s$  at zero without considering the derivative (or derivatives) of this variable. Accordingly, there are certainly variations in the sliding variable, though negligible, which cause the chattering phenomenon in the control signal. In the literature, there are several approaches to handle the phenomenon and to reduce the chattering effect. Especially, one of the approaches to deal with the chattering issue is the HOSMC, which provides a continuous control signal that drives not only the sliding variable

but also its derivatives to zero. In other words, the HOSMC attempts to synthesize the continuous control, and consequently, the chattering will be reduced. During the subsequent lines, we are just going to consider the special case of the HOSMC, called the SOSMC, which is one of the simplest in implementing and can eliminate the chattering phenomenon. Briefly, the main idea of the SOSMC is to drive the sliding variable and its derivative to zero, that is,  $s, \dot{s} \rightarrow 0$  in a finite-time. The SOSMC consists of several algorithms such as “sub-optimal algorithm”, “twisting algorithm”, “super twisting algorithm”, and so on. In this study, utilizing an integral state not requiring the information of  $\dot{s}$  in the control, we provide some different super twisting algorithms with the relative degree of 1, which are more effective than the SOSMCs. To this end and to drive the sliding variable  $s$  to zero in a finite-time, first we define the reaching term of the control input as follows:

$$u_{reach} = -\alpha|S_{fs}|^\rho \text{Sign}(S_{fs}) - \beta \int \text{Sign}(S_{fs}) dt. \quad (23)$$

Here,  $\alpha, \beta > 0$ ,  $0 < \rho < 1$ , and  $S_{fs}$  is given by (21). So, the continuous control law is determined as follows:

$$u = e_{eq} - \alpha|S_{fs}|^\rho \text{Sign}(S_{fs}) - \beta \int \text{Sign}(S_{fs}) dt. \quad (24)$$

By substituting (6) with (24), the fuzzy super-twist control (FSTC) law is described by

$$u = -f(X, t) - \sum_{i=1}^{n-1} \lambda_i e_{i+1} + x_d^{(n)}(t) - \alpha|S_{fs}|^\rho \text{Sign}(S_{fs}) - \beta \int \text{Sign}(S_{fs}) dt. \quad (25)$$

The following properties are presented by the super-twisting control (STC) formulation in (25):

- The STC in (25) is an SOSMC, since it drives both  $s, \dot{s} \rightarrow 0$  in a finite-time.
- The STC in (25) is continuous, since both terms  $\alpha|S_{fs}|^\rho \text{Sign}(S_{fs})$  and  $\beta \int \text{Sign}(S_{fs}) dt$  are continuous. Now, the high-frequency switching term is hidden under the integral.

The FSTC plant is shown in Fig. 8.

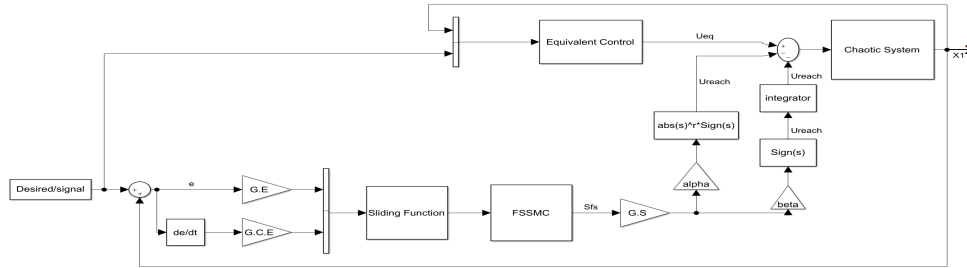


Figure 8: Scheme of the FSTC

**Theorem 4.1.** Assume the uncertain chaotic system in (1) controlled by  $u$  in (25) with  $\alpha|\xi_1|^\rho - F_{max} - D_{max} \geq 0$ , where  $S_{fs}$  is defined in (21),  $0 < \rho < 1$ , and  $\alpha, \beta > 0$ . Then, the error state trajectory converges to the sliding surface  $S_{fs}(t) = 0$  in a finite-time.

*Proof.* In Approach D,  $\dot{S}_{fs}$  is defined as

$$\dot{S}_{fs} = \Delta f(X, t) + d(t) - \alpha|S_{fs}|^\rho \text{Sign}(S_{fs}) - \beta \int \text{Sign}(S_{fs}) dt. \quad (26)$$

The system in (26) can be equivalently developed by the following system of two first-order differential equations:

$$\begin{cases} \dot{\xi}_1 = -\alpha|\xi_1|^\rho \text{Sign}(\xi_1) + \Delta f(X, t) + d(t) + \xi_2, & \xi_1 = S_{fs}, \\ \dot{\xi}_2 = -\beta \text{Sign}(\xi_1). \end{cases} \quad (27)$$

A candidate Lyapunov function for the system is taken as  $V(\xi) = \beta|\xi_1| + \frac{1}{2}\xi_2^2$ . Then, to provide the global finite-time stability

$$\begin{aligned}
\dot{V} &= \beta \frac{\xi_1}{|\xi_1|} \dot{\xi}_1 + \dot{\xi}_2 \xi_2 \\
&= \beta \frac{\xi_1}{|\xi_1|} (-\alpha|\xi_1|^\rho \text{Sign}(\xi_1) + \Delta f(X, t) + d(t) + \xi_2) + \xi_2 (-\beta \text{Sign}(\xi_1)) \\
&= -\alpha\beta|\xi_1|^\rho + \beta \text{Sign}(\xi_1) \Delta f(X, t) + \beta \text{Sign}(\xi_1) d(t) + \beta \text{Sign}(\xi_1) \xi_2 - \beta \text{Sign}(\xi_1) \xi_2 \\
&\leq \beta(F_{\max} + D_{\max} - \alpha|\xi_1|^\rho) \\
&= -\beta(\alpha|\xi_1|^\rho - F_{\max} - D_{\max}).
\end{aligned} \tag{28}$$

Now, if  $\alpha|\xi_1|^\rho - F_{\max} - D_{\max} \geq 0$  we have  $\alpha|\xi_1|^\rho \geq F_{\max} + D_{\max}$ . Thus, (28) can be rewritten as follows:

$$\dot{V} \leq -\beta\alpha|\xi_1|^\rho = -c|\xi_1|^\rho,$$

wherein,  $c = \alpha\beta$ . Based on the definition of Lyapunov function we have  $|\xi_1| \leq \frac{1}{\beta}V$  therefore,  $\dot{V} \leq -c\frac{1}{\beta^\rho}V^\rho$  for  $0 < \rho < 1$ . Employing Lemma 2.1 gives the desired result.  $\square$

**Remark 4.2.** In this approach, to further weaken the chattering phenomenon, we may replace the function  $\text{Sign}(S_{fs})$  by  $\tanh(cS_{fs})$  function in (25). Hence, the new FSTC law is introduced as follows:

$$u = -f(X, t) - \sum_{i=1}^{n-1} \lambda_i e_{i+1} + x_d^{(n)}(t) - \alpha|S_{fs}|^\rho \tanh(c_1 S_{fs}) - \beta \int \text{Sign}(S_{fs}) dt, \tag{29}$$

where  $c_1$  is a positive constant.

## 5 Simulation results

In this section, we aim to verify the performances of the all suggested control laws, Approaches A–D, for the following multi-scroll chaotic system with a hysteresis nonlinear with the uncertainties and disturbances:

$$\begin{cases} \dot{x}_1 = x_2, \\ \dot{x}_2 = -ax_1 + bx_2 + a.k.hys(x_1) + \Delta f(X, t) + d(t) + u(t). \end{cases} \tag{30}$$

Here,  $X = [x_1, x_2] = [x, \dot{x}]$  stands for the state variable,  $a, b$ , and  $k$  are given constants, and  $hys(\cdot)$  is a hysteresis nonlinear function with extension to the third quadrant (Fig. 9 shows its transfer characteristic). Moreover,  $\Delta f(X, t)$  and  $d(t)$  are the uncertainties and disturbance terms, respectively. For the simulation, in the system in (30), we set  $\Delta f(X, t) = 0.1 \sin(x_1) \sin(x_2)$  and  $d(t) = 0.05 \cos(t)$ . Obviously,  $\Delta f(X, t) \leq F_{\max} = 0.1$  and  $d(t) \leq D_{\max} = 0.05$ . Fig. 10 shows the chaotic system in (30) according to Table 2,  $u(t) = 0$ , and without uncertainty and disturbance terms. Note that the uncontrolled uncertain system in (30) (i.e.  $u(t) = 0$ ) is also chaotic. By the former discussion, to design

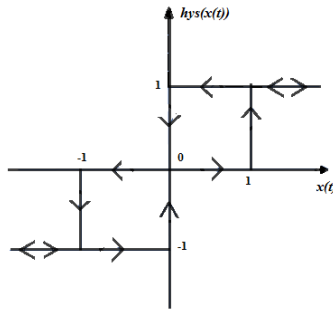


Figure 9: Transfer characteristic of  $hys(x(\cdot))$  function

an appropriate control law, the sliding variable is introduced as

$$s(t) = e_2(t) + \lambda e_1(t), \tag{31}$$

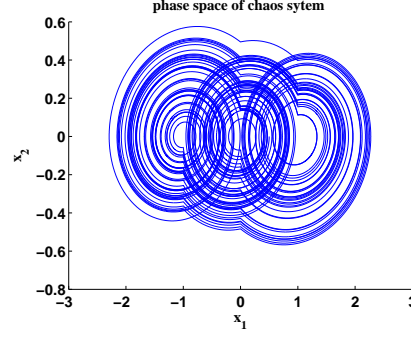


Figure 10: Phase plot of the chaotic attractor

Table 2: Parameters of system (30)

Parameter	Value	Parameter	Value
$x_1(0)$	0.5	a	0.15
$x_2(0)$	0	b	0.065
$F_{\max}$	0.1	k	1
$D_{\max}$	0.05	$\alpha$	2
$\lambda$	8	$\beta$	1.5
$\rho$	0.5	$c_1$	1
$c_2$	1		

where  $e_i(t) = x_i(t) - x_{di}(t)$  and  $x_{di}(t) = x_d^{(i-1)}(t)$ . Therefore, by solving  $\dot{s} = 0$ , we obtain the equivalent control as follows:

$$\dot{s}(t) = \dot{e}_2(t) + \lambda \dot{e}_1(t) = -ax_1 + bx_2 + a.k.hys(x_1) + u - \ddot{x}_d(t) + \lambda \dot{x}(t) - \lambda \dot{x}_d(t).$$

Thus, the equivalent control is obtained as

$$u_{eq} = ax_1 - bx_2 - a.k.hys(x_1) + \ddot{x}_d(t) - \lambda \dot{x}(t) + \lambda \dot{x}_d(t). \quad (32)$$

Hence, according to Approach A and (32), the control input is given by

$$u = ax_1 - bx_2 - a.k.hys(x_1) + \ddot{x}_d(t) - \lambda \dot{x}(t) + \lambda \dot{x}_d(t) - \bar{K} \tanh\left(\frac{s}{\Phi_{fs}}\right). \quad (33)$$

In the simulation, we choose  $x_d = \sin(t)$  as the target, which is a periodic orbit. Regarding (17) and Table 2, Fig. 11 demonstrates the time response of  $x_1$ , the state trajectory in phase plane, the time response of the sliding surface, the control action, and the time response of the error states for tracking  $x_d$ .

Now, in accordance with Approach B and (32), the control law is derived as

$$u = ax_1 - bx_2 - a.k.hys(x_1) + \ddot{x}_d(t) - \lambda \dot{x}(t) + \lambda \dot{x}_d(t) - K \tanh(S_{fs}). \quad (34)$$

The simulation results are shown in Fig. 12. Approach C and (32) yield the following control law:

$$u = ax_1 - bx_2 - a.k.hys(x_1) + \ddot{x}_d(t) - \lambda \dot{x}(t) + \lambda \dot{x}_d(t) - K \tanh\left(\frac{S_{fs}}{\Phi_{fs}}\right). \quad (35)$$

Fig. 13 illustrates the simulation results. From Approach D and (32), we have the following control law:

$$u = ax_1 - bx_2 - a.k.hys(x_1) + \ddot{x}_d(t) - \lambda \dot{x}(t) + \lambda \dot{x}_d(t) - \alpha |S_{fs}|^\rho \text{Sign}(S_{fs}) - \beta \int \text{Sign}(S_{fs}) dt, \quad (36)$$

and the results are displayed in Fig. 14.

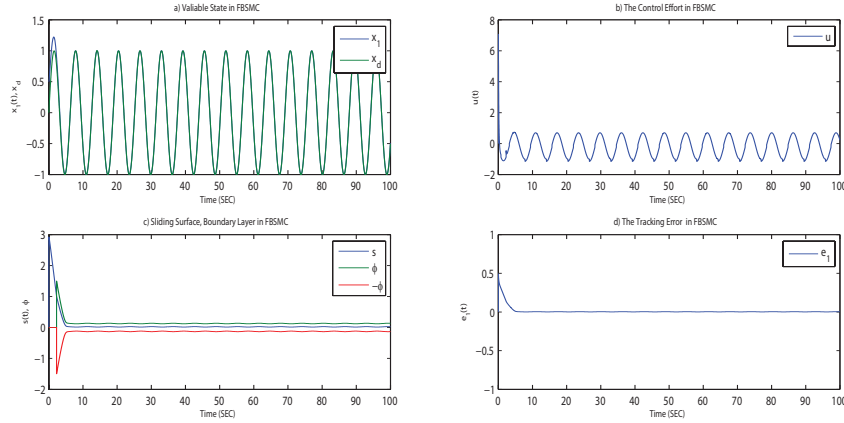


Figure 11: The simulation results according to Approach A for the system in (30): (a) Trajectories of the controlled system for  $x_d = \sin(t)$ . (b) Responses of the control action for tracking to the desired orbit. (c) Trajectories  $s(t)$  for the desired orbit. (d) Trajectories for the desired orbit.

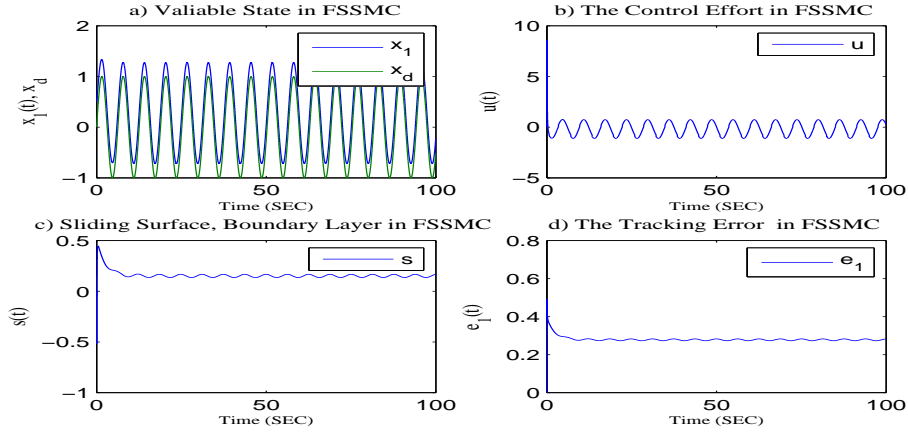


Figure 12: The simulation results according to Approach B for the system in (30): (a) Trajectories of the controlled system for  $x_d = \sin(t)$ . (b) Responses of the control action for desired orbit. (c) Trajectories  $s(t)$  for the desired orbit. (d) Trajectories of the error for the desired orbit.

For more comparison, we apply the proposed method (Approach D) on the Chen system in [31]:

$$\begin{aligned}
 \frac{dx_1}{dt} &= x_1, \\
 \frac{dx_2}{dt} &= x_3, \\
 \frac{dx_3}{dt} &= 130x_1 - 50x_2 - x_3 - x_1^3 + \Delta f + d(t) + u(t).
 \end{aligned}
 \tag{37}$$

$\Delta f$  is considered as the following sine signal:

$$\Delta f = 2 \sin(\pi x_1) \sin(\pi x_2) \sin(\pi x_3).$$

Table 3 gives the initial values and parameters setting of system (37). Fig. 15 illustrates the simulation results based on proposed method (Approach D) for system (37). This system also was investigated in [31]. The reported results in Fig. 15 shows that our method is well performed in known Chen system (37) and one can see that the error of state variable is tend to zero. Also, the sliding surface without chattering after about 2 seconds tends to zero. Moreover, the state variable  $x_1$  after about 4 seconds tend to desired signal similar to the results in [31].

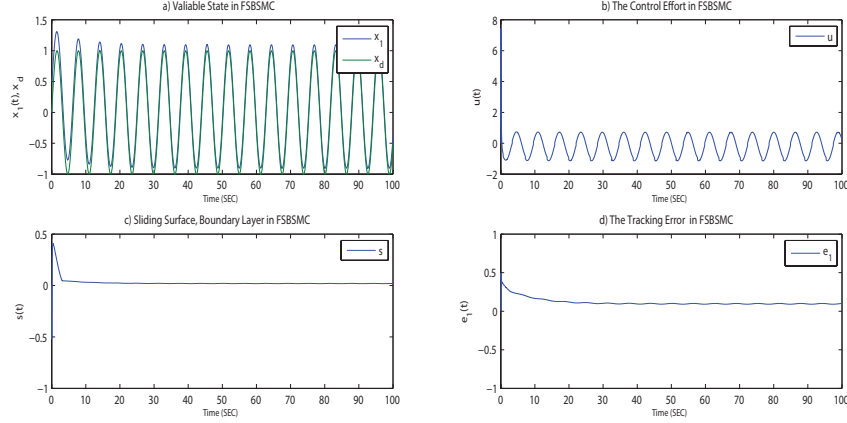


Figure 13: The simulation results according to Approach C for the system in (30): (a) Trajectories of the controlled system for  $x_d = \sin(t)$ . (b) Responses of the control action for desired orbit. (c) Trajectories  $s(t)$  for the desired orbit. (d) Trajectories of the error for the desired orbit.

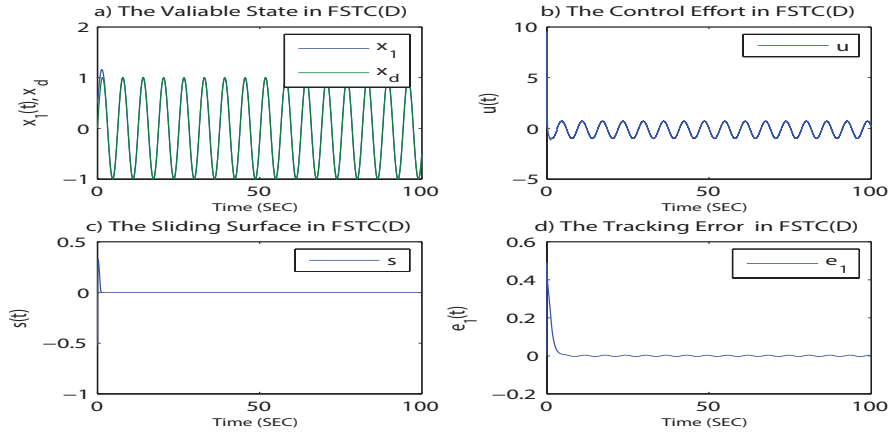


Figure 14: The simulation results according to Approach D for the system in (30): (a) Trajectories of the controlled system for  $x_d = \sin(t)$ . (b) Responses of the control action for desired orbit. (c) Trajectories  $s(t)$  for the desired orbit. (d) Trajectories of the error for the desired orbit.

Table 3: Parameters and initial values of system (37)

Parameter	Value	Parameter	Value
$x_1(0)$	5	$\lambda_1$	9.6201
$x_2(0)$	-2	$\lambda_2$	6.7014
$x_3(0)$	3	$c_1$	1
$D_{\max}$	5.7	$\alpha$	2.5
$c_2$	1	$\beta$	1.8
$\rho$	0.9		

## 6 Conclusion and discussion

For Approach A, the sliding surface reached zero after about 5 seconds and the control input was also smooth, as the simulation results are depicted in Fig. 11. In the next approach, Approach B, although the control input has no chattering, the tracking error (about 0.3) was not acceptable as the results given in Fig. 12. In order to improve the performance of the control action, two Approaches A and B were combined as Approach C to produce a new control law. Hence, the sliding surface converged to zero in less than 2 seconds with a lower overshoot than that of Approach

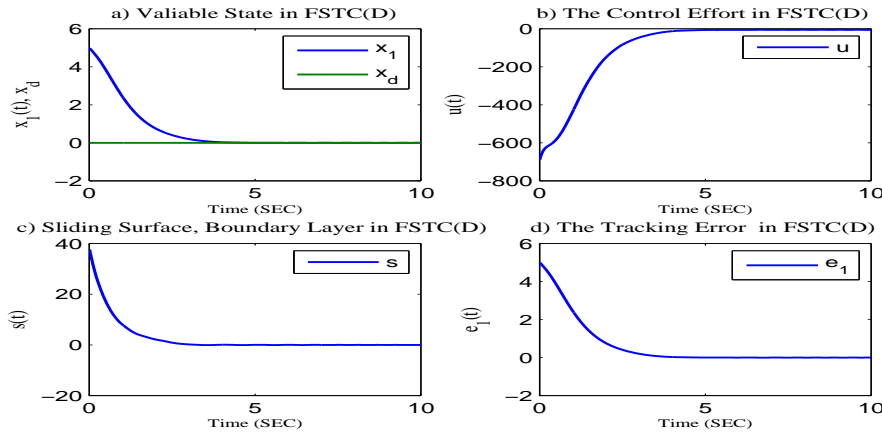


Figure 15: The simulation results according to Approach D for the system in (37): (a) Trajectories of the controlled system for  $x_d = 0$ . (b) Responses of the control action for desired orbit. (c) Trajectories  $s(t)$  for the desired orbit. (d) Trajectories of the error for the desired orbit.

A (see Fig. 13). By using the control law given in Approach D, the sliding surface convergence occurred earlier than Approach C, but unfortunately, even though the chattering effect was reduced, there still existed the chattering in the sliding surface and the control signal; while in [24], the sliding surface converged to zero in more than 10 seconds with overshoot in control, and moreover, the tracking error is bigger than this paper. By using Remark 4.2 as the simulation results were shown in Fig. 14, the chattering issue was reduced significantly and the error state was less than the previous approaches. Furthermore, we utilized the proposed method in known Chen system (37). One can check the method was well performed as depicted in Fig. 15. The reported results in Chen system was similar to the proposed method in [31]. Employing the developed method in some systems such as (30) and (37) demonstrated that the presented approach was well performed in chaotic systems.

In this work, several control laws based on the variable universe FSMC schemes for a class of uncertain chaotic systems were proposed. Moreover, by employing the Lyapunov technique, the finite-time stability of each proposed scheme was studied and proved in details. By applying the combinatorial methods, mentioned in Sections 3 and 4, the advantages of the fuzzy logic control and the SMC (the first-order and the second-order) were used simultaneously. The explained methods in Approaches A–D are more efficient than the previous ones such that the last one was proposed as the best control law. As expected, the simulation results illustrated the efficiency and high accuracy of these developed control laws in reduction and elimination of the chattering phenomenon, stability, and high speed in reach to sliding surface.

Some future research study based on this work may be suggested as follows. These approaches may be applied for hyper-chaotic systems, the membership can be chosen as nonlinear function, and the fuzzified sliding surface and boundary layer with super twist algorithm can be combined. Also, the gain of control can be considered as fuzzy.

## References

- [1] M. P. Aghababa, B. Hashtarkhani, *Synchronization of unknown uncertain chaotic systems via adaptive control method*, Journal of Computational and Nonlinear Dynamics, **10**(5) (2015), 051004.
- [2] V. Behnamgol, A. R. Vali, I. Mohammadzaman, *Second-order sliding mode control with finite-time convergence*, Amirkabir International Journal of Science and Research (Modeling, Identification, Simulation and Control), **45**(2) (2013), 41-52.
- [3] A. Boubellouta, A. Boulkroune, *Intelligent fractional-order control-based projective synchronization for chaotic optical systems*, Soft Computing, **23**(14) (2018), 5367-5384.
- [4] W. J. Chang, Q. Hong-Yu, K. Cheung-Chieh, *Sliding mode fuzzy control for nonlinear stochastic systems subject to pole assignment and variance constraint*, Information Sciences, **432** (2018), 133-145.
- [5] W. J. Chang, F. L. Hsu, *Sliding mode fuzzy control for Takagi–Sugeno fuzzy systems with bilinear consequent part subject to multiple constraints*, Information Sciences, **327** (2016), 258-271.



- [6] L. Chaouech, M. Soltani, A. Chaari, *Design of robust fuzzy Sliding-Mode control for a class of the Takagi–Sugeno uncertain fuzzy systems using scalar Sign function*, Iranian Journal of Fuzzy Systems, **17**(5) (2020), 97-107.
- [7] W. Chen, R. Zhang, L. Zhao, H. Wang, Z. Wei, *Control of chaos in vehicle lateral motion using the sliding mode variable structure control*, Journal of Automobile Engineering, **233**(4) (2019), 776-789.
- [8] Y. Ding, X. Wang, Y. Bai, N. Cui, *Global smooth sliding mode controller for flexible air-breathing hypersonic vehicle with actuator faults*, Aerospace Science and Technology, **92** (2019), 563-578.
- [9] L. Fang, T. Li, Z. Li, R. Li, *Adaptive terminal sliding mode control for anti-synchronization of uncertain chaotic systems*, Nonlinear Dynamics, **74**(4) (2013), 991-1002.
- [10] C. C. Fuh, H. H. Tsai, W. H. Yao, *Combining a feedback linearization controller with a disturbance observer to control a chaotic system under external excitation*, Communications in Nonlinear Science and Numerical Simulation, **17**(3) (2012), 1423-1429.
- [11] I. M. Ginarsa, A. Soeprijanto, M. H. Purnomo, *Controlling chaos and voltage collapse using an ANFIS-based composite controller-static var compensator in power systems*, International Journal of Electrical Power and Energy Systems, **46** (2013), 79-88.
- [12] N. Gnanesan, K. Chinnasamy, S. Ramasamy, Q. Zhu, *Robust exponential stability analysis for stochastic systems with actuator faults using improved weighted relaxed integral inequality*, IEEE Transactions on Systems, Man, and Cybernetics: Systems, **51**(6) (2021), 3346-3357.
- [13] S. Heidarzadeh, H. Salarieh, *A chattering-free finite-time robust synchronization scheme for uncertain chaotic systems*, Iranian Journal of Science and Technology: Transactions of Mechanical Engineering, **43**(8) (2018), 995-1003.
- [14] W. Ji, J. Qiu, H. R. Karimi, *Fuzzy-model-based output feedback sliding mode control for discrete-time uncertain nonlinear systems*, IEEE Transactions on Fuzzy Systems, **28**(8) (2020), 1519-1530.
- [15] B. Jiang, H. R. Karimi, S. Yang, Y. Kao, C. Gao, *Takagi–Sugeno model-based reliable sliding mode control of descriptor systems with semi-markov parameters: Average dwell time approach*, IEEE Transactions on Systems, Man, and Cybernetics: Systems, **51**(3) (2021), 1549-1558.
- [16] S. Khari, Z. Rahmani, B. Rezaie, *Designing fuzzy logic controller based on combination of terminal sliding mode and state feedback controllers for stabilizing chaotic behaviour in rod-type plasma torch system*, Transactions of the Institute of Measurement and Control, **38**(2) (2015), 150-164.
- [17] S. Khari, Z. Rahmani, B. Rezaie, *Controlling chaos based on a novel intelligent integral terminal sliding mode control in a rod-type plasma torch*, Chinese Physics B, **25**(5) (2016), 050201.
- [18] G. H. Li, *Projective synchronization of chaotic system using backstepping control*, Chaos, Solitons and Fractals, **29** (2006), 490-494.
- [19] H. Li, *Adaptive fuzzy controllers based on variable universe*, Science in China Series E-Technological Sciences, **29** (1999), 10-20.
- [20] H. Li, X. Liao, C. Li, C. Li, *Chaos control and synchronization via a novel chatter free sliding mode control strategy*, Neurocomputing, **74**(17) (2011), 3212-3222.
- [21] S. Lin, W. Zhang, *Chattering reduced sliding mode control for a class of chaotic systems*, Nonlinear Dynamics, **93**(4) (2018), 2273-2282.
- [22] H. Medhaffar, M. Feki, N. Derbel, *Stabilization of chaotic systems via fuzzy time-delayed controller approach*, Iranian Journal of Fuzzy Systems, **16**(2) (2019), 17-29.
- [23] J. Ni, L. Liu, C. Liu, X. Hu, T. Shen, *Fixed-time dynamic surface high-order sliding mode control for chaotic oscillation in power system*, Nonlinear Dynamics, **86** (2016), 401-420.
- [24] Y. J. Niu, X. Y. Wang, *A novel adaptive fuzzy sliding-mode controller for uncertain chaotic systems*, Nonlinear Dynamics, **75**(3) (2013), 1201-1209.

- [25] E. Ott, C. Grebogi, J. A. Yorke, *Controlling chaos*, Physical Review Letters, **64**(11) (1990), 28-37.
- [26] S. Park, H. Lee, S. Han, J. Lee, *Disturbance-observer-based fuzzy terminal sliding mode control for MIMO uncertain nonlinear systems*, International Journal of Control, Automation and Systems, **16** (2018), 1-14.
- [27] Z. Rahmani, B. Rezaie, M. H. Vali, *Designing a neuro-sliding mode controller for networked control systems with packet dropout*, International Journal of Engineering, **29**(4) (2016), 490-499.
- [28] S. Ramasamy, Y. H. Joo, *Passivity-based fuzzy ISMC for wind energy conversion systems with PMSG*, IEEE Transactions on Systems, Man, and Cybernetics: Systems, **51**(4) (2021), 2212-2220.
- [29] S. Ramasamy, G. Nagamani, T. Radhika, *Further results on dissipativity criterion for markovian jump discrete-time neural networks with two delay components via discrete Wirtinger inequality approach*, Neural Processing Letters, **45** (2017), 939-965.
- [30] S. Ramasamy, D. Song, Y. H. Joo, *T-S fuzzy-based sliding mode controller design for discrete-time nonlinear model and its applications*, Information Sciences, **519** (2020), 183-199.
- [31] B. Rezaie, S. Khari, *Adaptive intelligent terminal sliding mode controller for stabilizing a chaotic plasma torch system*, Journal of Vibration and Control, to appear, (2020), Doi: 10.1177/1077546320959520.
- [32] M. Roopaei, M. Zolghadri, S. Meshksar, *Enhanced adaptive fuzzy sliding mode control for uncertain nonlinear systems*, Communications in Nonlinear Science and Numerical Simulation, **14** (2009), 3670-3681.
- [33] A. Saghafinia, H. W. Ping, M. N. Uddin, *Fuzzy sliding mode control based on boundary layer theory for chattering-free and robust induction motor drive*, The International Journal of Advanced Manufacturing Technology, **71** (2014), 57-68.
- [34] M. Sarailoo, Z. Rahmani, B. Rezaie, *Fuzzy sliding mode control for hyper chaotic chen system*, Advances in Electrical and Computer Engineering, **12**(1) (2012), 85-90.
- [35] J. Slotine, W. Li, *Applied nonlinear control*, Prentice-Hall, New Jersey, 1991.
- [36] A. Vahidi-Moghaddam, A. Rajaei, M. Ayati, *Disturbance-observer-based fuzzy terminal sliding mode control for MIMO uncertain nonlinear systems*, Applied Mathematical Modelling, **70** (2019), 109-127.
- [37] M. Van, H. J. Kang, Y. S. Suh, *A novel fuzzy second-order sliding mode observer controller for a T-S fuzzy system with an application for robot control*, International Journal of Precision Engineering and Manufacturing, **14**(10) (2013), 1703-1711.
- [38] Y. Wang, Y. Gao, H. R. Karimi, H. Shen, Z. Fang, *Sliding mode control of fuzzy singularly perturbed systems with application to electric circuit*, IEEE Transactions on Systems, Man, and Cybernetics: Systems, **48**(10) (2018), 1667-1675.
- [39] H. Wang, Z. Z. Han, Q. Y. Xie, W. Zhang, *Sliding mode control for chaotic systems based on LMI*, Communications in Nonlinear Science and Numerical Simulation, **14**(4) (2009), 1410-1417.
- [40] L. Wang, C. L. Philip Chen, *Adaptive fuzzy dynamic surface control of nonlinear constrained systems with unknown virtual control coefficients*, IEEE Transactions on Fuzzy Systems, **28**(8) (2020), 1737-1747.
- [41] G. Wang, J. Wu, B. Zeng, Z. Xu, X. Ma, *A chattering-free sliding mode control strategy for modular high-temperature gas-cooled reactors*, Annals of Nuclear Energy, **133** (2019), 688-695.
- [42] D. Q. Wei, X. S. Luo, *Passivity-based adaptive control of chaotic oscillations in power system*, Chaos Solitons and Fractals, **31** (2007), 665-671.
- [43] P. Zhou, P. Zhu, *A practical synchronization approach for fractional-order chaotic systems*, Nonlinear Dynamics, **89** (2017), 1719-1726.
- [44] M. M. Zirkohi, T. C. Lin, *Interval type-2 fuzzy neural network indirect adaptive sliding mode control for an active suspension system*, Nonlinear Dynamics, **79** (2015), 513-526.